

Diketopyrrolopyrrole-based polymer:fullerene nanoparticle films with thermally stable morphology for organic photovoltaic applications

Natalie P. Holmes, Centre for Organic Electronics, University of Newcastle, University Drive, Callaghan NSW 2308, Australia

Ben Vaughan, Centre for Organic Electronics, University of Newcastle, University Drive, Callaghan NSW 2308, Australia; CSIRO Energy Technology, P. O. Box 330, Newcastle 2300, Australia

Evan L. Williams, Institute of Materials Research and Engineering (IMRE), Agency for Science, Technology, and Research (A*STAR), 2 Fusionopolis Way, Singapore 138634, Singapore

Renee Kroon, and **Mats R. Andersson**, Ian Wark Research Institute, University of South Australia, Mawson Lakes Campus, SA 5095, Australia; Department of Chemical and Biological Engineering/Polymer Technology, Chalmers University of Technology, 41296 Göteborg, Sweden

A.L. David Kilcoyne, Lawrence Berkeley National Laboratory, Advanced Light Source, Berkeley, CA 94720, USA

Prashant Sonar, Institute of Materials Research and Engineering (IMRE), Agency for Science, Technology, and Research (A*STAR), 2 Fusionopolis Way, Singapore 138634, Singapore; School of Chemistry, Physics and Mechanical Engineering, Queensland University of Technology (QUT), Brisbane 4000, Australia

Xiaojing Zhou, **Paul C. Dastoor**, and **Warwick J. Belcher**, Centre for Organic Electronics, University of Newcastle, University Drive, Callaghan NSW 2308, Australia

Address all correspondence to Natalie P. Holmes at natalie.holmes@newcastle.edu.au

(Received 2 December 2016; accepted 23 January 2017)

Abstract

Polymer:fullerene nanoparticles (NPs) offer two key advantages over bulk heterojunction (BHJ) films for organic photovoltaics (OPVs), water-processability and potentially superior morphological control. Once an optimal active layer morphology is reached, maintaining this morphology at OPV operating temperatures is key to the lifetime of a device. Here we study the morphology of the PDPP-TNT (poly(3,6-dithiophene-2-yl-2,5-di(2-octyldodecyl)-pyrrolo[3,4-c]pyrrole-1,4-dione-*alt*-naphthalene)):PC₇₁BM ([6,6]-phenyl C₇₁ butyric acid methyl ester) NP system and then compare the thermal stability of NP and BHJ films to the common poly(3-hexylthiophene) (P3HT): phenyl C₆₁ butyric acid methyl ester (PC₆₁BM) system. We find that material T_g plays a key role in the superior thermal stability of the PDPP-TNT:PC₇₁BM system; whereas for the P3HT:PC₆₁BM system, domain structure is critical.

Plastic solar cells are receiving increasing attention as a renewable energy option due to their flexibility for diverse applications, ability to be printed economically on a mass-scale, and the fast improvements in power conversion efficiency that are being reported by the research community.^[1,2] Currently in the plastic solar cell research field four key focuses include: (a) lowering the material band gap in order to harvest a larger portion of the solar spectrum,^[3,4] (b) tuning the blend morphology such that the donor and acceptor material domains are of a similar size as the exciton diffusion length,^[2,5] (c) investigating means of printing the photoactive materials from environmentally friendly solvents,^[6,7] and (d) improving the stability of the photoactive layer to both photochemical and morphological degradation.^[8,9] Here we report a nanoparticle (NP) photoactive layer prepared from the low band gap polymer PDPP-TNT [poly(3,6-dithiophene-2-yl-2,5-di(2-octyldodecyl)-pyrrolo[3,4-c]pyrrole-1,4-dione-*alt*-naphthalene)] and fullerene acceptor phenyl C₇₁ butyric acid methyl ester (PC₇₁BM) that seeks to address all four of these criteria. That is, PDPP-TNT possesses an optical band gap of 1.5 eV,^[4] NPs have been fabricated from PDPP-TNT (in a blend with PC₇₁BM) that enable films to be

spin coated from water-based inks, and the NP films are morphologically stable under thermal stress, with the maximum conditions tested being 130 °C for 60 min and 150 °C for 10 min.

NP photoactive layers represent a new and interesting option for tailoring the donor–acceptor (D–A) domain size at the nanoscale. The semiconductor material domain sizes can be controlled prior to film deposition by altering particle size, as well as post-deposition by applying thermal annealing treatments. While considerable effort is invested by the wider research community into optimizing the nanoscale morphology of interpenetrating donor and acceptor materials in organic photovoltaic (OPV) photoactive layers [whether they be solution-cast bulk heterojunction (BHJ) or nanoparticulate], it is also recognized that stable materials and morphology are required for the long-term operation of the solar cells; especially given that a common degradation process in OPV devices is gross phase separation of pure material domains.^[10,11] A simple method of gauging morphological stability is heating the photoactive layer to 85 °C (the maximum standard OPV operating temperature),^[12] or above, and checking for signs of morphological degradation. The excellent photochemical, mechanical,

and thermal stability reported for DPP-based materials makes them a promising option, and has led to their extensive use as high-performance pigments in paints, plastics, and inks.^[13]

Initial reports of the use of DPP-based polymers in NPs for OPV applications have shown encouraging results for this new material system.^[7,14] However, these studies did not investigate the morphology of the NPs beyond that of simple imaging of the film surface. The correct phase separation within the photoactive layer, more specifically the size and purity of the donor and acceptor material domains, is crucial to the successful function of that layer in an OPV device.^[5] In addition, once the photoactive layer morphology has been optimized, the susceptibility of this morphology to thermal degradation during OPV operation is of paramount importance to the lifetime of solar cells. This paper investigates the morphology of PDPP-TNT:PC₇₁BM NP layers, and the subsequent stability of these layers to morphological degradation.

PDPP-TNT:PC₇₁BM NPs were fabricated with a blend ratio of 1:2 donor:acceptor material using the miniemulsion method reported previously.^[15] A summary of this method is provided in Electronic Supplementary Information. A 1:2 donor:acceptor ratio was chosen as it had previously been reported as the optimized ratio for DPP-based polymer:PC₇₁BM BHJ OPVs.^[16–19] The NP size and size distribution were measured by applying a circular Hough transform algorithm to scanning electron microscopy (SEM) images of spin coated NP films (Fig. S1) giving a mean particle diameter of 113 ± 42 nm and a median of 106 nm.

Near-edge X-ray absorption fine structure (NEXAFS) spectroscopy was utilized in order to determine key absorption energies of PDPP-TNT and PC₇₁BM. The NEXAFS spectra of PDPP-TNT and PC₇₁BM are presented in Fig. S2 in Electronic Supplementary Information. An energy of 284.5 eV for PC₇₁BM and both 285.2 and 287.8 eV for PDPP-TNT were chosen for compositional mapping of the PDPP-TNT:PC₇₁BM NP films using scanning transmission X-ray microscopy (STXM). PDPP-TNT:PC₇₁BM 1:2 NPs were spin coated onto silicon nitride (Si₃N₄) window membrane substrates, and then rastered with respect to the incident beam to produce X-ray absorption images at the three energies. More detail on the STXM and NEXAFS measurements performed at the Advanced Light Source on beamline 5.3.2.2 can be found in the Electronic Supplementary Information. SVD (singular value decomposition) fitting was performed to generate composition maps for PDPP-TNT and PC₇₁BM, these are presented in Figs. 1(a) and 1(b) for as-cast NPs, with matching transmission electron microscopy (TEM) [Fig. 1(c)] performed on a Jeol JEM-1011 TEM. A core-shell NP morphology was observed for all sizes of PDPP-TNT:PC₇₁BM NPs imaged, down to the resolution of the STXM instrument. The STXM compositional maps were used to calculate the PDPP-TNT and PC₇₁BM concentrations in the two NP domain types, with the NP shells being rich in polymer (70–85% PDPP-TNT) and the NP cores rich in fullerene (74–96% PC₇₁BM).

Thermal annealing is a widely used tool for making modifications to the morphology of as-cast organic semiconductor

films in a controlled way.^[11] Various thermal annealing treatment conditions were applied to the PDPP-TNT:PC₇₁BM NP films and the resultant morphology was investigated using STXM and TEM. The annealing conditions included 130 °C for 10 min [Figs. 1(d)–1(f)], 130 °C for 60 min [Figs. 1(g)–1(i)] and 150 °C for 10 min (Fig. 2). Each thermal treatment effectively sintered the NPs together (most clearly observed in the matching TEM images shown in Figs. 1 and 2 where NP polymer-rich shells join together), but the overall core-shell intra-particle morphology remained intact; resulting in a morphology beneficial for charge transport through the bulk film to the electrodes.^[15]

The annealing study was then repeated on additional PDPP-TNT:PC₇₁BM NP films spin cast onto conductive silicon substrates and the morphology investigated via SEM on a Zeiss Sigma ZP FESEM (see Electronic Supplementary Information for more detail on sample preparation). The SEM data presented in Fig. 3 for all three annealing conditions confirms the result obtained from STXM and TEM; the PDPP-TNT:PC₇₁BM NP films are largely stable to annealing at these conditions, with only subtle joining (sintering) of the NPs observed. This result is significant in comparison with other OPV material systems, such as the commonly utilized poly(3-hexylthiophene) (P3HT): phenyl C₆₁ butyric acid methyl ester (PC₆₁BM) system, where even mild annealing conditions can lead to gross phase separation of pure material domains.^[6,15]

Comparing the morphology of solution-cast (BHJ) and NP films

We now consider the morphology of the PDPP-TNT:PC₇₁BM NP film in the context of state-of-the-art OPV photoactive layers. The key requirements of an OPV photoactive layer are to have nanoscale donor and acceptor domains for effective exciton separation, as well as bicontinuous percolation pathways of both donor and acceptor material for holes and electrons, respectively, to reach the device electrodes.^[5] It is greatly beneficial if this optimal morphology can be easily achieved with simple processing, and if it can be achieved by casting the semiconductor materials from water-based inks this is even more advantageous.

For the ubiquitous P3HT:PC₆₁BM material system, casting films from chloroform solvent leads to a finely blended morphology^[20] [see atomic force microscopy (AFM) in Fig. 4(d)-inset], in such a case thermal or solvent annealing treatments need to be applied to promote some degree of phase separation to achieve donor and acceptor material domain sizes in the exciton diffusion length range (~10 nm).^[21] Interestingly, casting the same two materials from a higher boiling point solvent, such as trichlorobenzene (B.P. 214 °C), results in a mildly phase separated morphology with D–A material domain size at ~20 nm.^[22] The reason behind this morphology difference with casting solvent is thought to be the slower rate of solvent evaporation of the high boiling point solvent, meaning the two materials have more time to de-mix and form ordered

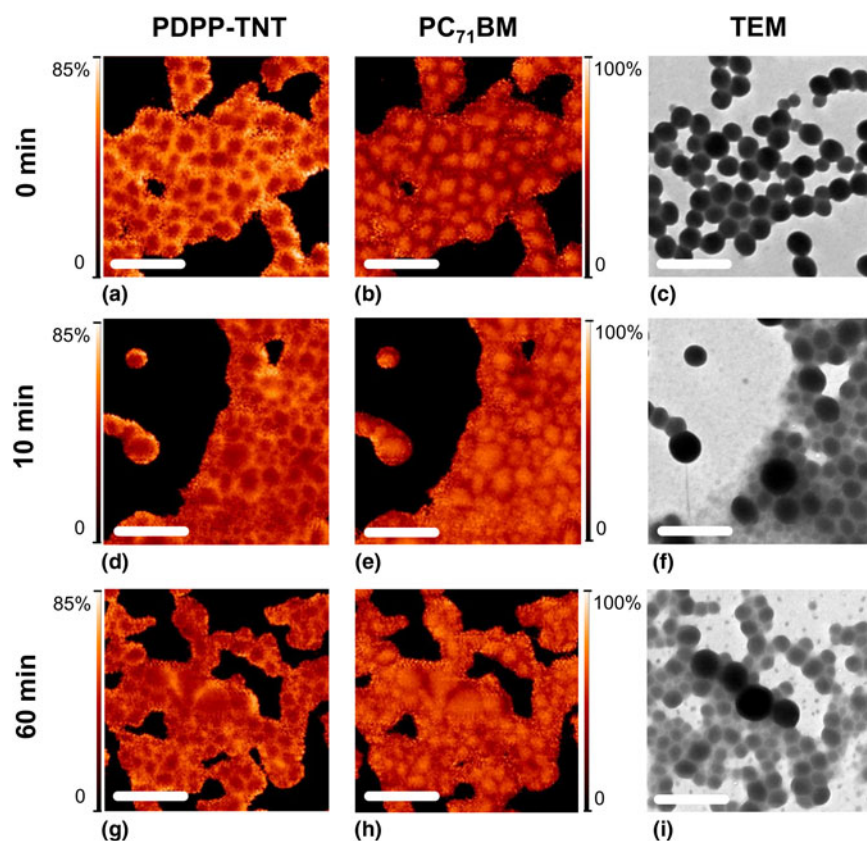


Figure 1. STXM fractional composition maps showing the concentration of PDPP-TNT (left column) and PC₇₁BM (middle column), with matching TEM (right column) in spin-coated 1:2 PDPP-TNT:PC₇₁BM NPs (a–c) as-cast (0 min), (d–f) annealed at 130 °C for 10 min, and (g–i) annealed at 130 °C for 60 min. All scale bars are 600 nm. The color contrast is scaled such that light colors correspond to higher component concentrations. Minima and maxima for the color scale are black = 0 and white = 100%, with the exception of (a), (d), and (g) where white is set to 85% for a clearer visualization of morphology.

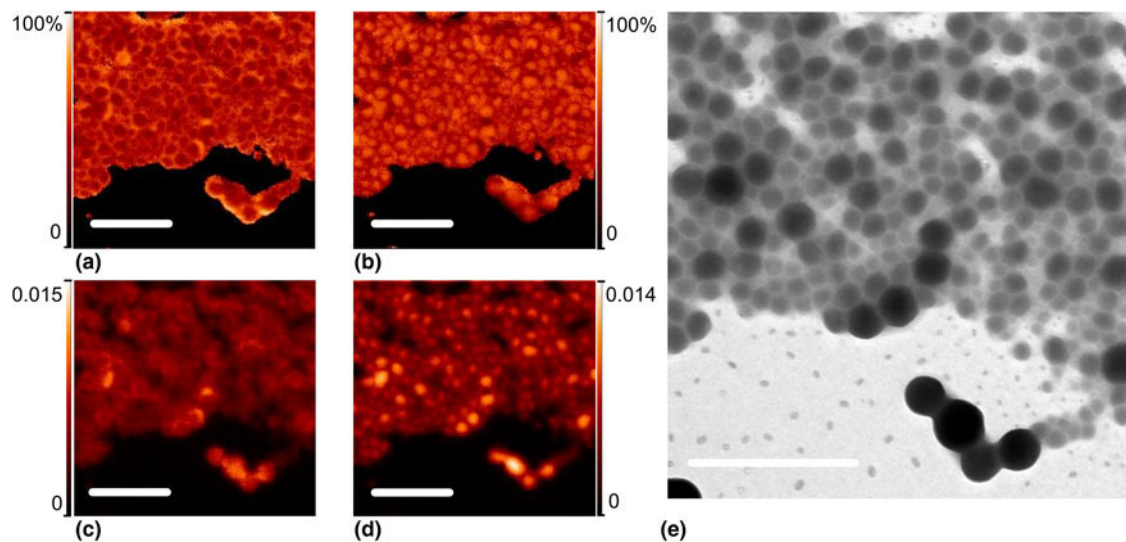


Figure 2. STXM fractional composition maps showing the concentration of (a) PDPP-TNT and (b) PC₇₁BM, with (c, d) corresponding STXM mass plots and (e) matching TEM for 1:2 PDPP-TNT:PC₇₁BM NPs annealed at 150 °C for 10 min. All scale bars are 1 μm. The color contrast is scaled such that light colors correspond to higher component concentrations. Minima and maxima for the color scale bar in (a) and (b) are black = 0 and white = 100%. For (c) and (d) the color scale bars indicate concentration of component in mg/cm².

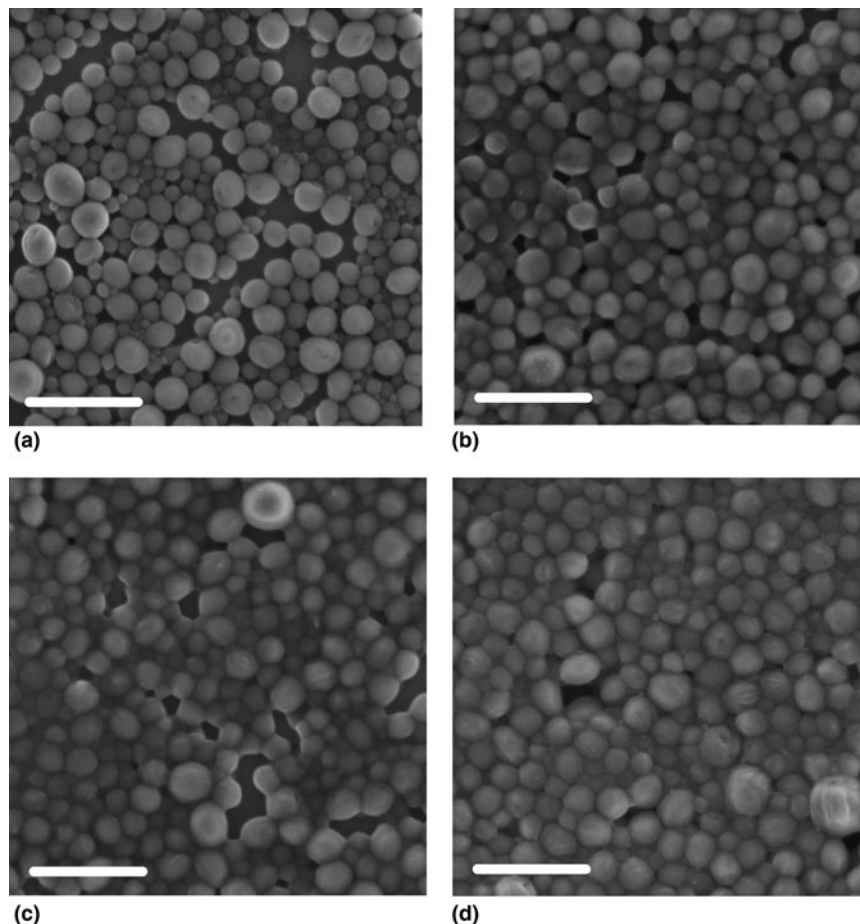


Figure 3. SEM of 1:2 PDPP-TNT:PC₇₁BM NP films (a) as-cast (0 min), (b) annealed at 130 °C for 10 min, (c) annealed at 130 °C for 60 min, and (d) annealed at 150 °C for 10 min. Scale bars are 600 nm.

domains.^[20] It is then of note that the opposite effect is observed for DPP-based polymer:PC₇₁BM blend films.^[23] Here, changing from a low boiling point solvent to a higher boiling point solvent results in a reduction of D–A material domain size, ~140 nm for chloroform (B.P. 61 °C), to ~50 nm for chlorobenzene (CB) (B.P. 131 °C), and 20–30 nm for dichlorobenzene (DCB) (B.P. 181 °C).^[23] For the case of a chloroform cast BJJ film of PDPP-TNT:PC₇₁BM, the morphology is cobblestone-like^[16] [see AFM in Fig. 4(b)-inset], consisting of PC₇₁BM-rich islands (200–500 nm in size) surrounded by PDPP-TNT polymer-rich valleys. Zoombelt et al.^[24] suggest that the large-scale morphology in some solvents can be attributed to a larger difference in solubilities of the polymer and fullerene. As the solvent evaporates, the fullerene crystallizes first, as the polymer stays solvated for longer, and then begins to aggregate.^[24] A similar trend is observed for other polymer systems, such as TQ1:PC₇₁BM, where a cobblestone-like film morphology also exists and the PC₇₁BM-rich islands vary in size from 400–800 to 200–400 to 50–100 nm for the solvents chloroform to CB to DCB, respectively.^[25] For both the PDPP-TNT

and TQ1 material systems, the use of additives has shown to be effective in optimizing film morphology, these have the effect of reducing the solubility of the polymer, hence forcing it to aggregate and precipitate sooner in the film-drying process.^[16,26] All of this work emphasizes the tedious yet necessary task of morphology optimization of the photoactive layers in BJJ OPV devices.

In comparison, semiconducting material NPs have the immediate advantage of allowing the morphology optimization to be decoupled from the solution casting stage of solar cell fabrication, in addition to enabling the photoactive layer to be printed from eco-friendly water-based inks. This is because the D–A domain sizes are pre-determined by the NP size, prior to casting the photoactive layer.^[6,15] The donor and acceptor domains in the PDPP-TNT:PC₇₁BM NPs studied in this paper are approaching the exciton diffusion length in size (20–50 nm PDPP-TNT-rich NP shells and 50–110 nm PC₇₁BM-rich NP cores) and can be further reduced by decreasing the NP size. The connected nature of the PDPP-TNT-rich NP shells following sintering is ideal for facilitating hole

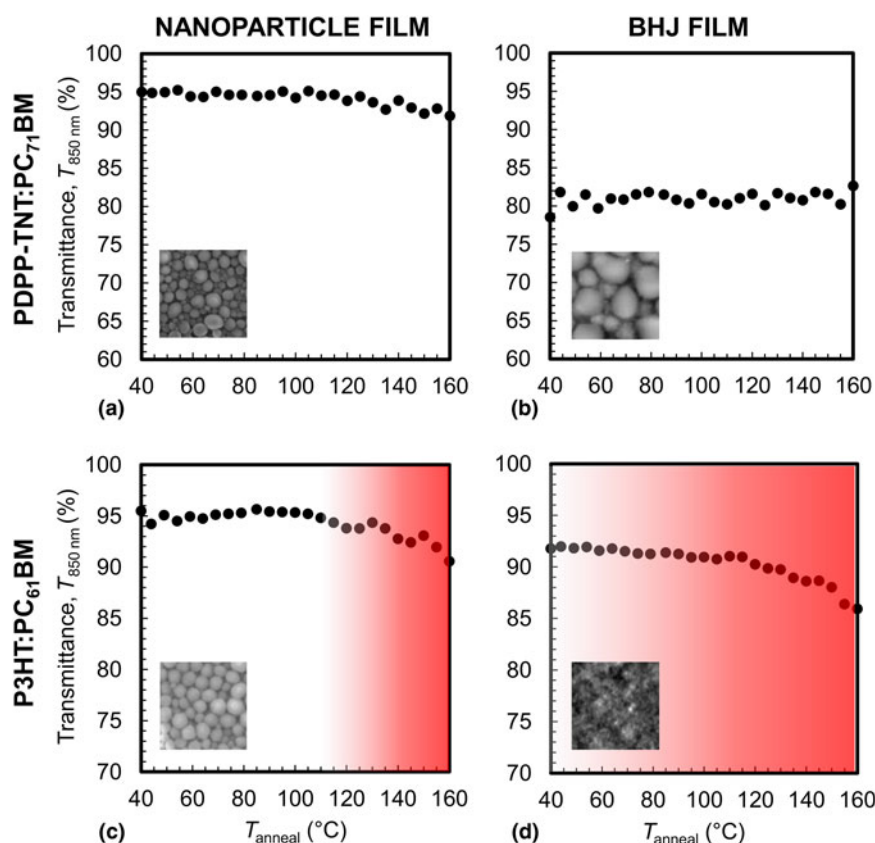


Figure 4. UV-vis transmittance plots of (a) PDPP-TNT:PC₇₁BM NP film, (b) PDPP-TNT:PC₇₁BM BHJ film (spin-cast from chloroform), (c) P3HT:PC₆₁BM NP film, and (d) P3HT:PC₆₁BM BHJ film (spin-cast from chloroform) exposed to a heating regime of 40 °C to 160 °C. Transmittance is a result of not only material absorption and film morphology (scattering), but also film thickness. Film thicknesses were: (a) 130 nm, (b) 225–230 nm, (c) 100 nm, and (d) 100 nm. The red shading in (c) and (d) indicates the temperature range where P3HT:PC₆₁BM films enter a regime in which the morphology can quickly become non-optimal as the material T_g s have been passed. The insets in (a) and (c) are SEM of the NP films prior to thermal treatment ($1 \times 1 \mu\text{m}^2$ area), and the insets in (b) and (d) are AFM height maps of the BHJ films prior to thermal treatment ($1 \times 1 \mu\text{m}^2$ area).

transport to the anode, while the small fraction of PC₇₁BM in the NP shells (15–30%) facilitates the transport of electrons through the bulk film to the cathode.

Morphological stability of blend films to thermal stress

The thermal stability of an organic semiconductor blend film is critical for its long-term use. Gradual evolution of the film nanostructure through phase separation and/or crystallization during operation is likely to affect the OPV device performance.^[11] If the material glass transition temperature (T_g) of the polymer:fullerene blend system is below the standard operating temperature of the solar cell, a change in blend film morphology is possible during operation, such as gross phase separation and the growth of micrometer-sized fullerene aggregates for binary systems of low thermodynamic miscibility. The T_g of organic semiconductor materials is often considered when choosing suitable thermal annealing conditions for the optimization of D–A blend film morphology, but the T_g must

also be considered relative to the maximum operating temperature of OPVs, which is reported to be 85 °C.^[12]

Although there are conflicting measurements of the T_g of P3HT,^[27] the value is generally accepted to be around room temperature. The T_g of PDPP-TNT is ~ 85 °C.^[7] Note though that the T_g of polymers can vary somewhat with molecular weight.^[28] The T_g of PC₆₁BM is reported to be 131 and 163 °C for PC₇₁BM.^[11] In addition, for two finely mixed materials only one T_g (intermediate between that of the individual components) will exist. This case is observed for a 1:1 P3HT:PC₆₁BM BHJ blend film cast from solvent, which is finely mixed, hence exhibiting a single T_g in the temperature range 40–60 °C.^[11,27,29]

An investigation of the relative thermal stability of four material films, namely PDPP-TNT:PC₇₁BM NP, PDPP-TNT:PC₇₁BM BHJ (spin-cast from chloroform solution), P3HT:PC₆₁BM NP, and P3HT:PC₆₁BM BHJ (spin-cast from chloroform solution), was undertaken using the method reported by Lindqvist et al.^[30] (procedure detailed in Electronic Supplementary Information). Here the UV-vis transmission of

each film is measured while heating from 40 to 160 °C and phase separation resulting in large fullerene aggregates is signaled by an increase in optical scattering and consequent reduction in transmitted light. The transmission plots for the four material films are presented in Fig. 4 (with full optical spectra of the material films at the initial thermal treatment (40 °C) and following the final thermal treatment (160 °C) available in Electronic Supplementary Information—Fig. S3). The P3HT:PC₆₁BM NPs were prepared in a similar manner to the PDPP-TNT:PC₇₁BM NPs, with the method reported in our previous paper^[15] and summarized in the Electronic Supplementary Information for this paper. For the PDPP-TNT:PC₇₁BM BHJ film [Fig. 4(b)] the UV–vis transmission was relatively invariant over the temperature range applied, indicating that the film is resistant to morphological degradation, as there is little to no increase in light scattering commonly attributed to the formation of micron-sized PCBM crystallites. A slight systematic decrease in transmittance is observed above ~120 °C for the PDPP-TNT:PC₇₁BM NP film [Fig. 4(a)]; however, no concomitant change in NP morphology is observed in the microscopy. At higher temperatures [130 °C (Fig. 1) and 150 °C (Fig. 2)] we do observe the gradual formation of small features on the Si₃N₄ substrate upon heating, which we hypothesize is due to the aggregation of surfactant; resulting in the observed minor decrease in transmission. Overall these results are in agreement with the STXM and electron microscopy data presented in Figs. 1–3 for the PDPP-TNT:PC₇₁BM NP system, where no morphological degradation was observed for the various thermal annealing treatments applied.

By contrast, for the P3HT:PC₆₁BM material system significant reductions in transmission are observed for both the NP and BHJ films upon heating. In the case of the P3HT:PC₆₁BM NP film [Fig. 4(c)], a systematic reduction of transmittance is observed from 110 °C which accelerates from approximately 130–140 °C. For the corresponding BHJ film [Fig. 4(d)], we observe a slight systematic decrease in transmittance from 40 to 110 °C. At 110 °C the rate of the decrease in transmittance increases until a total reduction of ~7% is observed at 160 °C [Fig. 4(d)] with optical microscopy confirming the formation of Micron-sized fullerene aggregates.

When comparing the PDPP-TNT:PC₇₁BM results to that of the P3HT:PC₆₁BM material system we hypothesize that the latter is less stable due to the lower T_g of both P3HT and PC₆₁BM compared with that of PDPP-TNT and PC₇₁BM. Although there are several factors that affect morphological evolution in these thin films (such as relative crystallinity of the two fullerenes), for the temperature range investigated here (40–160 °C), many of these factors (such as PC₇₁BM crystallization) are not activated until the T_g of PC₇₁BM (163 °C) is exceeded (e.g., the temperature required for crystallization in PC₇₁BM). As such, we speculate that T_g is an important activation threshold for morphological evolution in these complex thin films. This concept is further strengthened by the fact that the inferior stability of the P3HT:PC₆₁BM BHJ film compared with that of the P3HT:PC₆₁BM NP film can be attributed to a blend T_g of the BHJ

film of 40–60 °C.^[11,29] Thus, for the temperature range explored here, the BHJ system very quickly becomes mobile (rubbery state) and gross phase separation occurs. By contrast, the P3HT:PC₆₁BM NP film is not finely mixed as it is comprised fullerene-rich core domains and polymer-rich shell domains^[15] and hence does not exhibit a single low blend T_g .^[31] Therefore, the onset of gross phase separation for the P3HT:PC₆₁BM NP system will be at a higher temperature than for the BHJ system. Moreover, the semicrystalline nature of the P3HT in the shells of the P3HT:PC₆₁BM NPs [evidenced by P3HT vibronic peaks^[6] in the UV–vis spectrum Fig. S3(c)–40 °C] further stabilizes this system, as only the amorphous, disordered polymer fraction in the NP shells will display a glass transition.^[11] By contrast, the absence of any vibronic structure in the P3HT component of the UV–vis spectrum for the P3HT:PC₆₁BM BHJ film following the 40 °C thermal treatment [Fig. S3(d)] provides strong evidence that this film is mixed on a fine scale, with no crystalline P3HT domains. The blend T_g of this BHJ film is then passed quickly and micron-sized fullerene aggregates grow, resulting in the reduced transmittance [Fig. 4(d)], and the P3HT forms crystalline domains, evidenced by the appearance of strong P3HT vibronic peaks in the UV–vis spectrum measured after the final thermal treatment at 160 °C [Fig. S3(d)]. Indeed, it is clear from the UV–vis spectra in Fig. S3 that for the four film types, the P3HT:PC₆₁BM BHJ film underwent the most change during the thermal treatment regime.

Overall this is a promising result for the PDPP-TNT:PC₇₁BM NP material system, showing that the nanoscale domain size established pre-film deposition is stable to morphological degradation at standard OPV operating conditions. Furthermore, these results reveal that for the P3HT:PC₆₁BM system the NP films are more thermally stable than their BHJ counterparts, most importantly at the standard maximum operating conditions (85 °C). The results indicate that nanoparticulate material systems offer potential for the fabrication of thermally stable OPV devices and highlight the relevance of material T_g and domain composition to material stability.

Supplementary material

The supplementary material for this article can be found at <https://doi.org/10.1557/mrc.2017.3>.

Acknowledgments

The authors thank the University of Newcastle Electron Microscopy and X-ray Unit. Special thanks to Robin Arnold and Samson Dowland at the University of Sydney (Anatomy and Histology, School of Medical Sciences) where TEM measurements were performed. The University of Newcastle and the Australian Renewable Energy Agency (ARENA) are gratefully acknowledged for PhD scholarships (NH). We acknowledge financial support from the Commonwealth of Australia through the Access to Major Research Facilities Program. The A.L.S. is supported by the Director, Office of Science, Office of Basic Energy Sciences, of the U.S. Department of

Energy under Contract No. DE-AC02-05CH11231. This work was performed in part at the Materials node (Newcastle) and the Queensland node of the Australian National Fabrication Facility (ANFF), which is a company established under the National Collaborative Research Infrastructure Strategy to provide nano- and microfabrication facilities for Australia's researchers.

References

- M.M. Wienk, M. Turbiez, J. Gilot, and R.A.J. Janssen: Narrow bandgap diketopyrrolo-pyrrole polymer solar cells: the effect of processing on the performance. *Adv. Mater.* **20**, 2556 (2008).
- W. Li, K.H. Hendriks, A. Furlan, W.S.C. Roelofs, M.M. Wienk, and R.A.J. Janssen: Universal correlation between fibril width and quantum efficiency in diketopyrrolopyrrole-based polymer solar cells. *J. Am. Chem. Soc.* **135**, 18942 (2013).
- E. Zhou, Q. Wei, S. Yamakawa, Y. Zhang, K. Tajima, C. Yang, and K. Hashimoto: Diketopyrrolopyrrole-based semiconducting polymer for photovoltaic device with photocurrent response wavelengths up to 1.1 μm . *Macromolecules* **43**, 821 (2010).
- P. Sonar, S.P. Singh, Y. Li, Z.-E. Ooi, T. Ha, I. Wong, M.S. Soh, and A. Dodabalapur: High mobility organic thin film transistor and efficient photovoltaic devices using versatile donor-acceptor polymer semiconductor by molecular design. *Energy Environ. Sci.* **4**, 2288 (2011).
- F. Liu, Y. Gu, J.W. Jung, W.H. Jo, and T.P. Russell: On the morphology of polymer-based photovoltaics. *J. Polym. Sci. B: Polym. Phys.* **50**, 1018 (2012).
- N.P. Holmes, S. Ulum, P. Sista, K.B. Burke, M.G. Wilson, M.C. Stefan, X. Zhou, P.C. Dastoor, and W.J. Belcher: The effect of polymer molecular weight on P3HT:PCBM nanoparticulate organic photovoltaic device performance. *Sol. Energy Mater. Sol. Cells* **128**, 369 (2014).
- B. Vaughan, E.L. Williams, N.P. Holmes, P. Sonar, A. Dodabalapur, P. C. Dastoor, and W.J. Belcher: Water-based nanoparticulate solar cells using a diketopyrrolopyrrole donor polymer. *Phys. Chem. Chem. Phys.* **16**, 2647 (2014).
- C. Lindqvist, J. Bergqvist, O. Bäcke, S. Gustafsson, E. Wang, E. Olsson, O. Inganäs, M.R. Andersson, and C. Müller: Fullerene mixtures enhance the thermal stability of a non-crystalline polymer solar cell blend. *Appl. Phys. Lett.* **104**, 153301 (2014).
- A. Guerrero and G. Garcia-Belmonte: Recent advances to understand morphology stability of organic photovoltaics. *Nano-Micro Lett.* **9**, 10 (2016).
- S. Bertho, G. Janssen, T.J. Cleij, B. Conings, W. Moons, A. Gadisa, J. D'Haen, E. Goovaerts, L. Lutsen, J. Manca, and D. Vanderzande: Effect of temperature on the morphological and photovoltaic stability of bulk heterojunction polymer:fullerene solar cells. *Sol. Energy Mater. Sol. Cells* **92**, 753 (2008).
- C. Müller: On the glass transition of polymer semiconductors and its impact on polymer solar cell stability. *Chem. Mater.* **27**, 2740 (2015).
- M.O. Reese, S.A. Gevorgyan, M. Jørgensen, E. Bundgaard, S.R. Kurtz, D. S. Ginley, D.C. Olson, M.T. Lloyd, P. Morvillo, E.A. Katz, A. Elschner, O. Haillant, T.R. Currier, V. Shrotriya, M. Hermenau, M. Riede, K. R. Kirov, G. Trimmel, T. Rath, O. Inganäs, F. Zhang, M. Andersson, T. Tvingstedt, M. Lira-Cantu, D. Laird, C. McGuinness, S. Gowrisankar, M. Pannone, M. Xiao, J. Hauch, R. Steim, D.M. DeLongchamp, R. Rösch, H. Hoppe, N. Espinosa, A. Urbina, G. Yaman-Uzunoglu, J.-B. Bonekamp, A.J.J.M. van Breemen, C. Girotto, E. Voroshazi, and F. C. Krebs: Consensus stability testing protocols for organic photovoltaic materials and devices. *Sol. Energy Mater. Sol. Cells* **95**, 1253 (2011).
- A.B. Tamayo, B. Walker, and T.-Q. Nguyen: A low band gap, solution processable oligothiophene with a diketopyrrolopyrrole core for use in organic solar cells. *J. Phys. Chem. C* **112**, 11545 (2008).
- N.A.D. Yamamoto, M.E. Payne, M. Koehler, A. Facchetti, L.S. Roman, and A.C. Arias: Charge transport model for photovoltaic devices based on printed polymer:fullerene nanoparticles. *Sol. Energy Mater. Sol. Cells* **141**, 171 (2015).
- N.P. Holmes, N. Nicolaidis, K. Feron, M. Barr, K.B. Burke, M. Al-Mudhaffer, P. Sista, A.L.D. Kilcoyne, M.C. Stefan, X. Zhou, P. C. Dastoor, and W.J. Belcher: Probing the origin of photocurrent in nanoparticulate organic photovoltaics. *Sol. Energy Mater. Sol. Cells* **140**, 412 (2015).
- E.L. Williams, S. Gorelik, I. Phang, M. Bosman, C. Vijila, G. S. Subramanian, P. Sonar, J. Hobley, S.P. Singh, H. Matsuzaki, A. Furube, and R. Katoh: Nanoscale phase domain structure and associated device performance of organic solar cells based on a diketopyrrolopyrrole polymer. *RSC Adv.* **3**, 20113 (2013).
- K.H. Hendriks, G.H.L. Heintges, V.S. Gevaerts, M.M. Wienk, and R.A. J. Janssen: High-molecular-weight regular alternating diketopyrrolopyrrole-based terpolymers for efficient organic solar cells. *Angew. Chem.* **52**, 8341 (2013).
- L. Dou, J. Gao, E. Richard, J. You, C.-C. Chen, K.C. Cha, Y. He, G. Li, and Y. Yang: Systematic investigation of benzodithiophene- and diketopyrrolopyrrole-based low-bandgap polymers designed for single junction and tandem polymer solar cells. *J. Am. Chem. Soc.* **134**, 10071 (2012).
- W. Li, W.S.C. Roelofs, M.M. Wienk, and R.A.J. Janssen: Enhancing the photocurrent in diketopyrrolopyrrole-based polymer solar cells via energy level control. *J. Am. Chem. Soc.* **134**, 13787 (2012).
- M.T. Dang, G. Wantz, H. Bejbouji, M. Urien, O.J. Dautel, L. Vignau, and L. Hirsch: Polymeric solar cells based on P3HT:PCBM: role of the casting solvent. *Sol. Energy Mater. Sol. Cells* **95**, 3408 (2011).
- C. Nicolet, D. Deribew, C. Renaud, G. Fleury, C. Brochon, E. Cloutet, L. Vignau, G. Wantz, H. Cramail, M. Geoghegan, and G. Hadziioannou: Optimization of the bulk heterojunction composition for enhanced photovoltaic properties: correlation between the molecular weight of the semiconducting polymer and device Performance. *J. Phys. Chem. B* **115**, 12717 (2011).
- T. Wang, A.D.F. Dunbar, P.A. Staneic, A.J. Pearson, P.E. Hopkinson, J.E. MacDonald, S. Lilliu, C. Pizzey, N.J. Terrill, A.M. Donald, A.J. Ryan, R.A.L. Jones, and D.G. Lidzey: The development of nanoscale morphology in polymer:fullerene photovoltaic blends during solvent casting. *Soft Matter* **6**, 4128 (2010).
- R. Badrou Aich, Y. Zou, M. Leclerc, and Y. Tao: Solvent effect and device optimization of diketopyrrolopyrrole and carbazole copolymer based solar cells. *Org. Electron.* **11**, 1053 (2010).
- A.P. Zoombelt, S.G.J. Mathijssen, M.G.R. Turbiez, M.M. Wienk, and R.A. J. Janssen: Small band gap polymers based on diketopyrrolopyrrole. *J. Mater. Chem.* **20**, 2240 (2010).
- R. Hansson, L.K.E. Ericsson, N.P. Holmes, J. Rysz, A. Opitz, M. Campoy-Quiles, E. Wang, M.G. Barr, A.L.D. Kilcoyne, X. Zhou, P. Dastoor, and M. Moons: Vertical and lateral morphology effects on solar cell performance for a thiophene-quinoxaline copolymer:PC70BM blend. *J. Mater. Chem. A* **3**, 6970 (2015).
- F. Liu, Y. Gu, C. Wang, W. Zhao, D. Chen, A.L. Briseno, and T.P. Russell: Efficient polymer solar cells based on a low bandgap semi-crystalline DPP polymer-PCBM blends. *Adv. Mater.* **24**, 3947 (2012).
- P.E. Hopkinson, P.A. Staneic, A.J. Pearson, A.D.F. Dunbar, T. Wang, A. J. Ryan, R.A.L. Jones, D.G. Lidzey, and A.M. Donald: A phase diagram of the P3HT:PCBM organic photovoltaic system: implications for device processing and performance. *Macromolecules* **44**, 2908 (2011).
- C. Müller, E. Wang, L.M. Andersson, K. Tvingstedt, Y. Zhou, M. R. Andersson, and O. Inganäs: Influence of molecular weight on the performance of organic solar cells based on a fluorene derivative. *Adv. Funct. Mater.* **20**, 2124 (2010).
- C. Bruner, F. Novoa, S. Dupont, and R. Dauskardt: Decohesion kinetics in polymer organic solar cells. *ACS Appl. Mater. Interfaces* **6**, 21474 (2014).
- C. Lindqvist, E. Wang, M.R. Andersson, and C. Müller: Facile monitoring of fullerene crystallization in polymer solar cell blends by UV-vis spectroscopy. *Macromol. Chem. Phys.* **215**, 530 (2014).
- N.P. Holmes, M. Marks, P. Kumar, R. Kroon, M.G. Barr, N. Nicolaidis, K. Feron, A. Pivrikas, A. Fahy, A. Diaz de Zerio Mendaza, A.L. D. Kilcoyne, C. Müller, X. Zhou, M.R. Andersson, P.C. Dastoor, W. J. Belcher: Nano-pathways: bridging the divide between water-processable nanoparticulate and bulk heterojunction organic photovoltaics. *Nano Energy* **19**, 495 (2016).